Extended Abstracts of the 2014 International Conference on Solid State Devices and Materials, Tsukuba, 2014, pp660-661

Hole Mobility Enhancements in Strained $In_xGa_{1-x}Sb$ Heterostructure PMOSFET

Pengying Chang[1, 2], Xiaoyan Liu[2]*, Lang Zeng[2], Gang Du[2]
[1]School of Electronic and Computer Engineering, Peking University, Shenzhen, 518055, China
[2]Key Laboratory of Microelectronic Devices and Circuits (MOE), Institute of Microelectronics, Peking University, Beijing, 100871, China
E-mail: xyliu@ime.pku.edu.cn

Abstract

In this work, hole mobility in strained $In_xGa_{1-x}Sb$ devices is computed with different heterostructures. Physical models are calibrated with experimental data. Our results suggest that hole mobility increases with InSb mole fraction, especially with biaxial compressive strain. Mobility degrades with the scaling down of body thickness. An insert of thin cap layer with wide bandgap is helpful to enhance hole mobility.

1. Introduction

Ⅲ-Ⅴ compound semiconductors are one of the most potential contenders for future high-speed, low-power logic application due to their high electron mobility [1]. However, as an indispensable part of CMOS, it is of great significance to pursue high mobility p-channel devices. Strain engineering in silicon, such as strained Si on relaxed SiGe buffer layer, or SiGe even pure Ge channel with caps has been successful in improving pMOSFETs performance [2-3]. More recently, the technique has been employed to strained InSb, GaSb and InGaSb based devices for enhancing hole mobility [4-6]. A detailed simulation is necessary to assess the performance with such heterostructures.

In this paper, we study the design of the single gate (SG) compressively strained $In_xGa_{1-x}Sb/Al_{0.8}Ga_{0.2}Sb$ heterostructure MOSFET using six band $k\cdot p$ method self-consistently with Poisson equations. The impact of InSb fraction including biaxial compressive strain, body thickness and cap layer thickness is investigated by physics-based modeling.

2. Simulation Methods

We consider heterostructures of $In_xGa_{1-x}Sb/Al_{0.8}Ga_{0.2}Sb$, in which the magnitude of biaxial strain can be adjusted by varying InSb fraction x. This system has exhibited outstanding hole mobility in the narrow band gap (NB) $In_xGa_{1-x}Sb$ channel, and has sufficient valence band offset (VBO) between the NB and wide bandgap (WB) $Al_{0.8}Ga_{0.2}Sb$ to confine the charge in the $In_xGa_{1-x}Sb$ channel. Accurate band structures with strain considered are obtained by solving the 6 band $k\cdot p$ Schrödinger and Poisson equations self-consistently. The grids in kx-ky plane are generated by adaptive grid algorithm [7]. Hole mobility is calculated using Kubo-Greenwood formula accounting for non-polar acoustic and optical phonons, polar optical phonons, surface roughness and alloy scatterings. For InSb and GaSb, deformation potentials and phonon energies needed for mobility calculation are taken from [8]. Simulation parameter values for $In_xGa_{1-x}Sb$ are linearly interpolated from InSb and GaSb parameter values, which makes our approach similar to SiGe modeling in Ref [9]. The parameters for scattering calculation are listed in Table I.

3. Results and Discussion

Fig.1 and Fig.2 show the comparison between simulated and experimental hole mobility for InSb [5] and GaSb [6] based devices, and inset figures illustrate the device structures. The calibration of the model is performed by keeping the material and phonon scattering parameters fixed, while adjusting SR parameters. Our simulations reproduce well the experiments, which verify our method. Band structure parameters, deformation potentials and phonon energies for $In_xGa_{1-x}Sb$ are linearly interpolated from InSb and GaSb, leaving only alloy disorder potential U_0 and SR parameters adjustable. For U_0 in SiGe alloys, a wide range of values has been reported in the literature (0.2~1eV). Similarly, this uncertainty leads to different combinations of Δ and U_0. We use values of 0.1, 0.3 and 0.4eV for U_0 to fitting the experiments, seen in Fig.3. It's suggested that more accurate experimental values for mobility and alloy model are needed.

Fig.4 shows hole mobility vs. InSb fraction x in relaxed (a) and strained (b) $In_xGa_{1-x}Sb/Al_{0.8}Ga_{0.2}Sb$ w/ and w/o alloy scattering, respectively. The larger the value of U_0 is, the more important the alloy scattering is. In relaxed case, alloy scattering leads to an asymmetric 'U' shaped mobility behavior with large U_0. While for strained case, mobility increases monotonously with InSb fraction except for very low x with tensile strain, and three combinations of values for U_0 and Δ make little difference to the total mobility when x<70%. Hence in the simulation below, we adopt the values of U_0=0.3eV and Δ=1nm. Fig.5 depicts hole mobility vs. Ns for x=30%, 50% and 70%. As seen in Fig.6, increasing compression leads to a larger splitting between the HH and LH bands with the HH being higher in energy and hence with greater occupancy. Because HH and LH mixing is reduced near the Γ point, the in-plane mass of HH gets lighter as the HH-LH splitting increases. This reduced mass is expected to give rise to higher mobility.

The dependency of mobility on sheet density is presented in Fig.7 for $In_{0.5}Ga_{0.5}Sb/Al_{0.8}Ga_{0.2}Sb$ devices with different body thickness. As T_B is scaled from 10nm to 3nm, mobility strongly decreases. The effect of T_B downscaling on the total mobility is shown in Fig.8. Strong mobility degradation with T_B in $In_{0.5}Ga_{0.5}Sb/Al_{0.8}Ga_{0.2}Sb$ devices is evident for all Ns values considered. Mobility decrease is particularly steep in strained devices. Nevertheless, mobility in strained devices is still better than that in relaxed cases for the whole range of T_B.

A buried channel design with a thin WB cap layer in order to isolate out the effects of surface roughness and charge in the dielectric on the inversion charge is widely used in Ⅲ-Ⅴ heterostructure devices. Fig.9 (a) illustrates the structure with $Al_{0.8}Ga_{0.2}Sb$ cap, and corresponding band profiles are plotted for weak and strong inversion in Fig.9 (b) and (c). Hole mobility in 5nm-thick $In_{0.5}Ga_{0.5}Sb$ w/o and w/ cap layer of 1nm, 2nm, and 3nm is presented in Fig.10. Hole mobility is significantly enhanced with cap layer. Due to the VBO of $In_{0.5}Ga_{0.5}Sb/Al_{0.8}Ga_{0.2}Sb$, hole inversion exists not only in the $In_{0.5}Ga_{0.5}Sb$ but also in the cap. When inversion becomes stronger, the fraction of holes in the low mobility cap increases which can degrade mobility, hence a thin cap is sufficient.

4. Conclusions

Hole mobility enhancements in $In_xGa_{1-x}Sb/Al_{0.8}Ga_{0.2}Sb$ can be achieved by increasing InSb fraction due to increased biaxial compression which can enlarge split between HH and LH and reduce effective mass. Meanwhile, an insert of thin wide gap cap layer between gate oxide and channel can reduce the interface effect and hence enhance hole mobility. Mobility degradation with T_B downscaling is severe in strained devices.

Acknowledgment

This work is supported by NKBRP 2011CBA00604, NSFC Grant No. 61306104, China Postdoctoral Science Foundation Grant No. 2013M540018, and NSFC Grant No. 61250014.

References

[1] Jesús A. del Alamo, *Nature* 479.7373 (2011): 317-323.

[2] Aberg I, Ni Chleirigh C, Hoyt J L. *TED*, 2006, 53(5): 1021-1029.
[3] Takagi S, et al. *Materials Science and Engineering: B*, 2006, 250-255.
[4] B. R. Bennett, et al. *Journal of Crystal Growth*, 2008: 47-53.
[5] Radosavljevic. M., et al. *IEDM, 2008.*
[6] Nainani Aneesh, et al. *IEDM, 2010*
[7] Pengying Chang, Xiaoyan Liu, et al, *IWCE*, 2014, accepted.
[8] http://www.ioffe.ru/SVA/NSM/
[9] Pham A T, et al. *TED*, 2007, 54(9): 2174-2182.

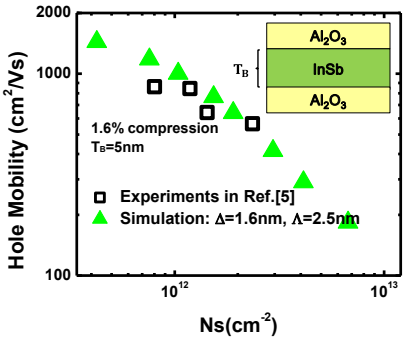

Fig.1 Calculated hole mobility for 5nm-thick compressively strained InSb-based devices and measurements by M.Radosavljevic [5].

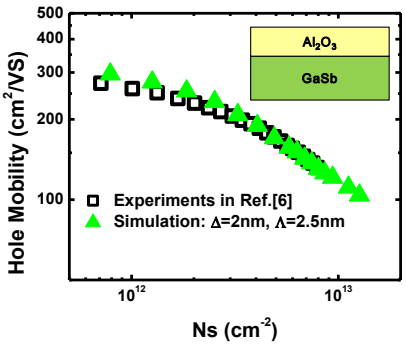

Fig.2 Comparison between simulated and experimental [6] hole mobility for GaSb inversion layer.

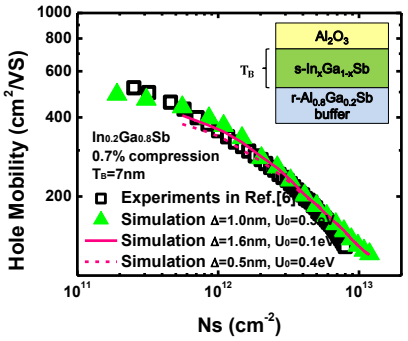

Fig.3 Hole mobility for a 7nm-thick $In_{0.2}Ga_{0.8}Sb$ with 0.7% compressive strain [6]. The numerical value of U_0 is extracted as a fitting parameter.

TABLE I SCATTERING PARAMETERS FOR ALL MECHANISMS USED IN SIMULATION

Parameters	Symbol	Unit	InSb	GaSb	$In_xGa_{1-x}Sb$		
Acoustic deformation potential	D_{ac}	eV	7.02	6.88	Linearly interpolated		
Optical deformation potential	$(DK)_{op}$	10^8eV/cm	10.81	11.03	Linearly interpolated		
Optical phonon energy	$\hbar\omega_{op}$	meV	25	29.8	Linearly interpolated		
Polar optical phonon energy	$\hbar\omega_{pop}$	meV	24.3	28.89	Linearly interpolated		
Surface correlation length	Δ	nm	1.6	2	1.6	1	0.5
Surface average height	Λ	nm	2.5	2.5	2.5		
Alloy scattering potential	U_0	eV			0.1	0.3	0.4

*For scattering calculation in A_xB_{1-x} alloys, there are three interpolation methods: (1) scattering rates are linearly interpolated; (2) the squared value of the deformation potentials are linearly interpolated; (3) the values of deformation potentials and phonon energies are linearly interpolated. We adopt the last method.

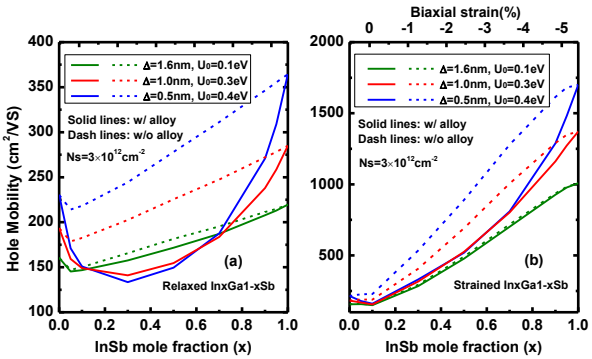

Fig.4 Hole mobility in 5nm relaxed (a) and strained (b) $In_xGa_{1-x}Sb$ grown on relaxed $Al_{0.8}Ga_{0.2}Sb$ buffer layer with sheet density of $3\times10^{12}cm^{-2}$ Results are obtained either including or neglecting the alloy scattering and plotted versus the InSb mole fraction x.

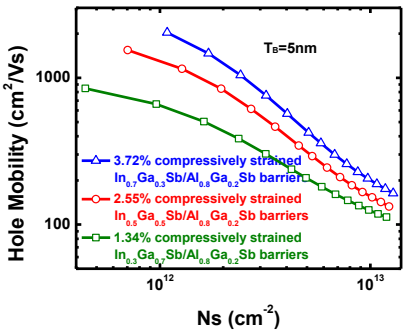

Fig.5 Hole mobility versus sheet density for 5nm-thick compressively strained $In_xGa_{1-x}Sb$ with x=0.3, 0.5 and 0.7, respectively, corresponding to 1.34%, 2.55% and 3.72% biaxial strain.

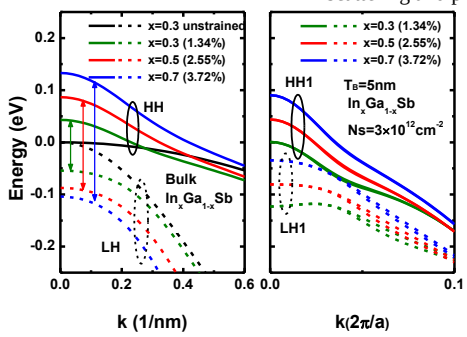

Fig.6 Band structures of $In_xGa_{1-x}Sb$ with x=0.3, 0.5 and 0.7 for bulk (left) and T_B=5nm (right). Biaxial compression lifts the degeneracy between the HH and LH, and reduces the effective mass of HH.

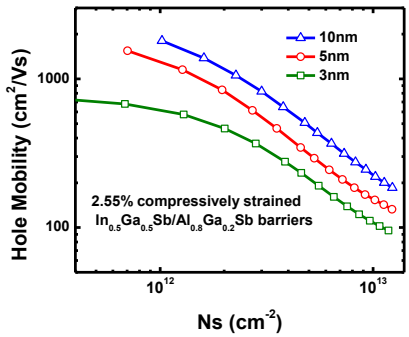

Fig.7 Hole mobility as a function of sheet density for 2.55% compressively strained $In_{0.5}Ga_{0.5}Sb$ with respect to T_B of 10nm, 5nm, and 3nm. Mobility decreases with the body thickness.

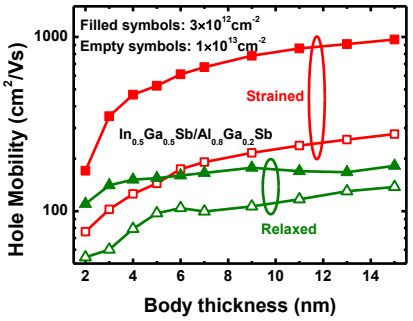

Fig.8 Hole mobility versus body thickness ranging from 2nm to 15nm for relaxed and strained $In_{0.5}Ga_{0.5}Sb/Al_{0.8}Ga_{0.2}Sb$, respectively. The sheet density is at $3\times10^{12}cm^{-2}$ and $1\times10^{13}cm^{-2}$.

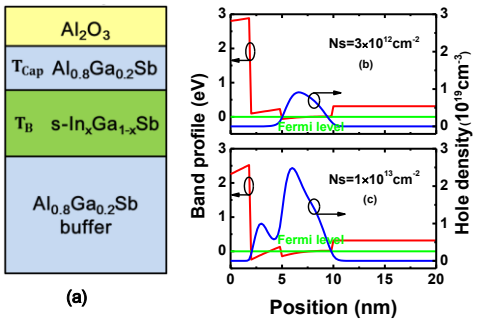

Fig.9 (a) Heterostrucutures of strained $In_xGa_{1-x}Sb$ devices with cap layer between oxide and channel. Band profiles in strained $In_{0.5}Ga_{0.5}Sb$ are plotted at weak and strong inversion in (b) and (c).

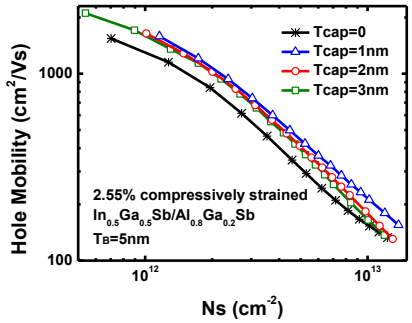

Fig.10 Hole mobility in 2.55% compressively strained $In_{0.5}Ga_{0.5}Sb$ without and with cap layer of 1nm, 2nm and 3nm is plotted. A thin WB cap is successful in enhancing hole mobility.